ACS OMEGA

http://pubs.acs.org/journal/acsodf

Article

Degradation of the Three-Phase Boundary Zone of Carbon Fiber Anodes in an Electrochemical System

Hongfang Sun, Wenpeng Liu, Jie Ren, Chao Wu, Feng Xing, Wei Liu, and Li Ling*

Cite This: *ACS Omega* 2023, 8, 26359−26368

Read Online

ACCESS | Metrics & More | Article Recommendations

ABSTRACT: The electrochemical recycling nanoarchitectonics of graphene oxide from carbon fiber reinforced polymers (CFRPs) is a promising approach due to its economic and environmental benefits. However, the rapid degradation of the CFRP anode during the recycling process reduces its overall efficiency. Although previous studies have investigated the electrochemical oxidation of carbon fibers (CFs) and bonding of CFs to the matrix, few researchers have explicitly studied the electrochemical activity of CFs and the possible fracture caused by strong electrochemical reactions. To address this gap, this study investigates the degradation mechanism of CF anodes by analyzing changes in overall mechanical properties, hardness, elastic modulus, functional groups, and elemental composition of individual fibers. The experimental results demonstrate that the three-phase boundary region experiences the most severe degradation, primarily due to the number of oxygen-containing functional groups, which is the most important factor affecting the degree of degradation. This continuous decrease in the hardness and elastic modulus of individual fibers eventually leads to the fracture of CF anodes.

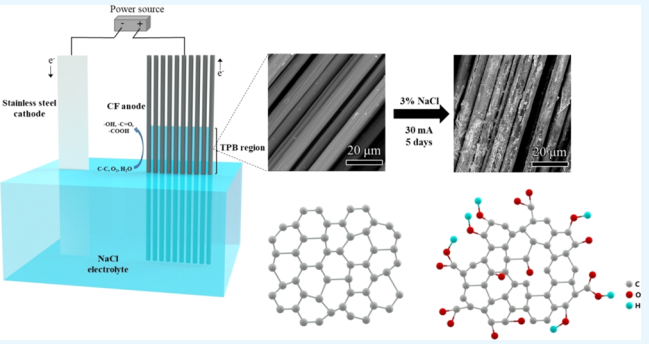

1. INTRODUCTION

In recent years, carbon fiber reinforced polymers (CFRPs) have found extensive applications in military, aviation, sports, racing, wind power, and civil engineering due to their ultrahigh specific strength and modulus.[1] Consequently, the increased usage of CFRPs has led to a corresponding increase in waste production. If not fully recycled, Europe and Asia are estimated to accumulate 190,000 and 149,000 tons of waste CFRPs by 2050, respectively.[2] Therefore, proper recycling of CFRPs has garnered significant attention.[3] However, simple mechanical recycling of waste CFRPs results in a considerable amount of carbon fiber (CF) waste, which is the key component of CFRPs.[4] To improve the efficiency of CFRP recycling, researchers have explored various recycling methods, among which electrochemical methods have great potential for recycling nanoarchitectonics of graphene oxide (GO) with high efficiency and low cost.[5,6] Nonetheless, during the electrochemical recycling process, the CFRP anode tends to degrade rapidly or even fracture.[6] The fracture of the CFRP leads to not only raw material waste but also suspension of the electrification process, thereby reducing overall recycling efficiency.

Several studies have made preliminary observations and explanations on the degradation of CFRPs in electrochemical systems,[7,8] attributing the degradation of CFRP anodes to the decomposition of resin fracture associated with C−N bonds in epoxy resins and the generation of new compounds due to the chemical reaction of CFs with the epoxy resin.[8,9] However, these papers only focused on the degradation of the overall tensile properties of CFRP anodes and the combination of the CF and matrix. Few comprehensive investigations have been conducted on the degradation mechanism of CF anodes, which could be beneficial in reducing the occurrence of CFRP anode fractures and improving the application efficiency of recycling waste CFRPs through electrochemical systems.

This paper investigates the degradation mechanisms of CF anodes based on changes in overall tensile properties, mechanical properties, functional groups, element content, functional group changes, and microscopic morphology under the influence of different current intensities and electrolyte concentrations in electrochemical systems. CF anodes are delineated into regions according to the degree of degradation, and the mechanisms related to the formation of highly corroded regions are investigated. The results of this paper provide effective theoretical support for avoiding anode fractures and better accelerating the oxidation of CFs in the

Received: April 27, 2023
Accepted: June 30, 2023
Published: July 13, 2023

https://doi.org/10.1021/acsomega.3c02900
ACS Omega 2023, 8, 26359−26368

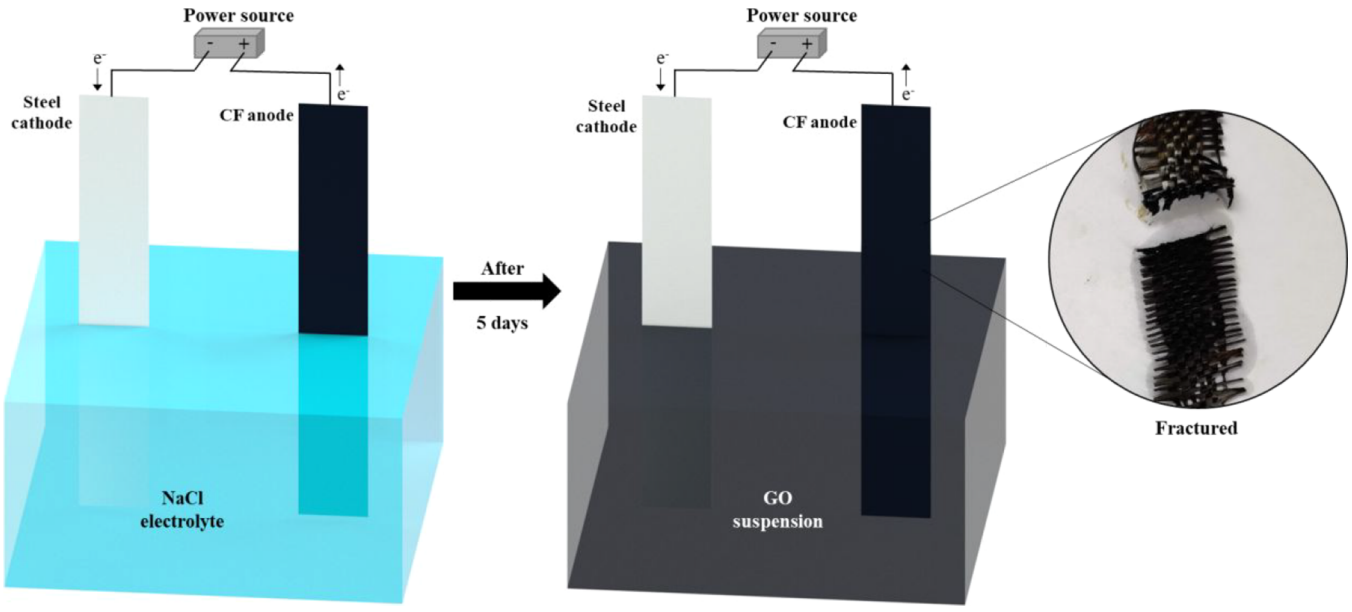

Figure 1. Schematic view of the electrochemical system employed in this study.

electrochemical system, which is of great help in improving the recycling efficiency of waste CFRPs.

2. EXPERIMENTAL INVESTIGATION

2.1. Materials and Electrochemical System Setup. The electrochemical system studied in this paper is shown in Figure 1, consisting of three parts: anode, cathode, and electrolyte. CFs produced by Guangzhou Caben Composite Co., Ltd. (CA.BEN), with a weight of 208 g/m^2 and a size of 200 (L) × 20 (W) × 0.22 (T) mm^3, were used as anodes. Stainless steel sheets with a size of 200 (L) × 15 (W) × 0.5 (T) mm^3 served as cathodes. The NaCl solution used as the electrolyte was prepared from NaCl powder produced by Xilong Chemical and deionized water.

In this study's electrochemical system, the horizontal distance between the CF anode and the stainless steel cathode was 50 mm, and the length of the part immersed below the liquid surface was 100 mm. The experimental energization currents were 4, 10, and 30 mA, corresponding to current densities of 1.0, 2.5, and 7.5 A/m^2 (relative to the area of the anode immersed in NaCl electrolyte). The concentrations of NaCl electrolytes used were 3, 10, and 20% to investigate the possible effects of current density and NaCl electrolyte concentration on the degradation of CF anodes. The current densities and concentration of NaCl electrolytes were chosen based on our previous research on recycling GO from CFs from CFRPs.[6] After 5 days of continuous electrification, the CF anodes were collected as test samples. Another set of CF anodes was soaked in NaCl solution with a concentration of 3% at the same depth for 5 days as control samples.

Details of the samples are listed in Table 1, and each sample is named according to the experimental conditions. For example, "I4S3" denotes that the applied current is 4 mA, and the concentration of NaCl electrolyte is 3%, while "I0S3" indicates that the CF anode is immersed in NaCl electrolyte with a concentration of 3%.

2.2. Testing Methods. In this study, the mechanical properties (tensile force, elongation at break, hardness, and maximum elastic modulus) of CF anode samples were tested

Table 1. Details of Samples

sample	current (mA)	current density (A/m^2)	concentration of NaCl electrolyte (%)
I0S3	0	0	3
I4S3	4	1.0	3
I10S3	10	2.5	3
I30S3	30	7.5	3
I4S10	4	1.0	10
I4S20	4	1.0	20

using tensile and nanoindentation tests. The changes in their functional groups and elemental compositions were analyzed by FTIR and energy-dispersive spectrometry (EDS) techniques.

An MTS Criterion 60.305 tensile tester produced by MTS Company was used for the tensile test. For fractured CF anodes, the region with the highest corrosion degree was selected to prepare the sample. Before the test, both ends of each sample were coated with epoxy resin and left at room temperature for 24 h to increase friction between the sample and the fixture. A tensile speed of 4 mm/min was used until the sample broke.

The nanoindentation test was performed using a nanoindentation accessory coupled with a scanning electron microscope. To avoid insufficient contact between the CF anode sample and the sample table, small pieces of the CF anode were cut and placed in low viscosity epoxy resin at room temperature for 24 h. Silicon carbide sandpapers (P600 and P1200) were used for rough polishing, followed by four kinds of abrasive pastes (14, 3.5, 1, and 0.25 μm) for fine polishing. The nanoindentation test of the polished samples was performed using the continuous stiffness method (CSM) with a strain rate of 0.5/s. Five measurements were taken for each sample, and the average value was expressed as the final test result.

The changes in functional groups of CF anodes were tested using Fourier transform infrared spectroscopy (FTIR). Before the test, 0.3 g of the dried sample and 30 g of KBr powder were ground by hand under an infrared baking lamp until the black

https://doi.org/10.1021/acsomega.3c02900
ACS Omega 2023, 8, 26359−26368

CF was completely invisible. Then, 0.05 g of the ground powder was pressed into a transparent sheet for FTIR testing using a Spectrum One FTIR spectrometer produced by PerkinElmer, with a test scanning range of 400−4000 cm^{-1} and a resolution of 2 cm^{-1}.

The energy-dispersive spectrometer in a scanning electron microscope was used to observe the surface morphology of the CF anode before and after degradation, and the oxygen element content was measured. A ProX EDS desktop scanning electron microscope produced by Phenom-World company was used for the test, with an accelerating voltage of 5 kV and a magnification of 4000×.

3. RESULTS AND DISCUSSION

3.1. Influence on Mechanical Properties. The degradation of CF anodes is most visibly shown through a decline in their mechanical properties. To assess this change, tensile and nanoindentation tests were conducted on the CF anodes after electrification.

3.1.1. Tensile Properties. The force−displacement curve and comparison data of maximum tensile force and elongation at break for CF anodes are presented in Figure 2. Maximum tensile force reflects a sample's resistance to tensile force, while elongation at break indicates its toughness.[10] Results indicate that the unenergized sample (I0S3) exhibited the largest maximum tensile force and elongation at break, indicating superior tensile performance and toughness. However, the tensile strength of CF anodes decreased to varying degrees, with the first place to break consistently several centimeters above the electrolyte surface in different samples. These findings suggest that mechanical property degradation primarily occurs in regions close to the electrolyte.

Figure 2a,c illustrates the force vs displacement curves of CF anodes as a function of current density when the NaCl electrolyte concentration was kept at 3%. Results indicate that when the current density was 1.0 A/m^2, the maximum tensile force of the CF anode decreased by only 12%, but the elongation at break sharply decreased by 63% compared to unenergized CF. When the current density increased to 2.5 A/m^2, the maximum tensile force of the CF anode remained relatively unchanged, but the elongation at break continued to decrease by 75%. However, when the current density increased to 7.5 A/m^2, the fibers on the CF anode were severely corroded or even fell off, leading to almost zero maximum tensile force data, and the sample was unable to bear the force. Moreover, Figure 2b,d shows the force vs displacement curves of CF anodes as a function of NaCl electrolyte concentration while maintaining the current density at 1.0 A/m^2. Results reveal that when the electrolyte concentration increased from 3 to 10%, the maximum tensile and elongation at break of the samples remained relatively constant. However, when the electrolyte concentration further increased from 10 to 20%, the decrease in the maximum tensile force significantly increased from 10 to 44%, although the elongation at break of the CF anode remained relatively unchanged.

The results indicate that current density is the most significant factor affecting the toughness of CF anodes in electrochemical systems. Even at extremely low current densities, the toughness of CF anodes significantly reduced after being connected to the electrochemical system, and the degree of degradation increases with increasing current density. Conversely, changes in NaCl electrolyte concentration have little effect on the toughness of CF anodes, and there appears

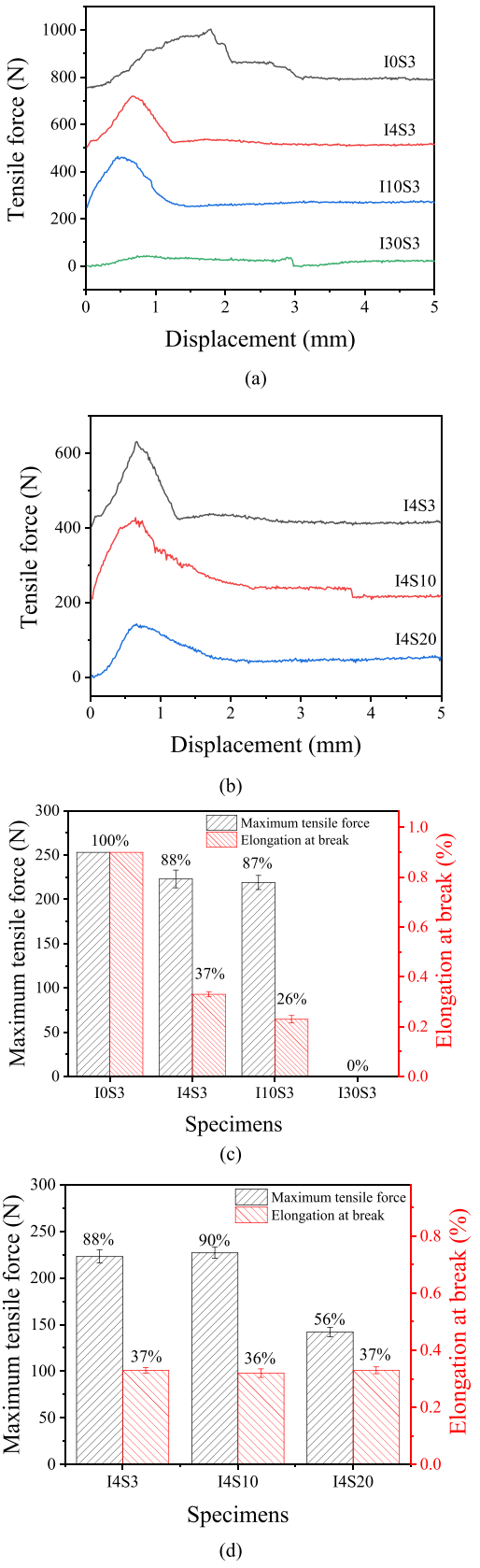

Figure 2. Tensile force vs displacement curves of CF anodes as a function of currents (a) and electrolyte concentrations (b) and maximum tensile force and elongation at break of CF anodes as a function of currents (c) and electrolyte concentrations (d).

https://doi.org/10.1021/acsomega.3c02900
ACS Omega 2023, 8, 26359−26368

to be no clear correlation between maximum tensile force and toughness. In electrochemical systems with very low current density and electrolyte concentration, CF anodes can maintain good maximum tensile force despite a sharp drop in toughness.

Therefore, further studies on the mechanical property degradation of individual fibers on CF anodes are necessary to fully explain the difference in the effects of current density and electrolyte concentration changes on the degradation of CF anodes in electrochemical systems.

3.1.2. Hardness and Elastic Modulus. To investigate the changes in mechanical properties during the degradation of CF anodes, the hardness and elastic modulus of individual fibers on CF anodes were tested using the nanoindentation accessory coupled with SEM after testing their tensile properties. Figure 3a shows the SEM image of the probe and the CF fixed with epoxy resin during the test. Results indicate that nanoindentation can precisely control the probe to test the physical properties of single fibers.

At a constant NaCl electrolyte concentration of 3%, the hardness and elastic modulus of the CF anode were measured in relation to current density (0−7.5 A/m^2) as shown in Figure 3b. Results indicate that at lower current densities (1.0 A/m^2), the CF anode experiences a 35% decrease in hardness and a 20% decrease in elastic modulus compared to unenergized CFs. As the current density increases to 2.5 and 7.5 A/m^2, the CF anode's hardness decreases by 52 and 75%, respectively, while its elastic modulus decreases by 26 and 66%, respectively. This suggests that increasing current density leads to a continued reduction in the CF anode's hardness, whereas the effect on elastic modulus is less pronounced at lower current densities (1.2 and 2.5 A/m^2).

The CF anode's hardness decreases more than its elastic modulus at various current densities. At a fixed current density of 1.0 A/m^2, the hardness and elastic modulus of the CF anode were measured as a function of NaCl electrolyte concentration (3−20%), as shown in Figure 3c. Results show that both properties decrease significantly with increasing NaCl concentration. At low concentrations (5%), the CF anode experiences a 35% decrease in hardness and a 20% decrease in elastic modulus compared to unenergized CFs. As NaCl concentration increases to 10 and 20%, the CF anode's hardness decreases by 50 and 67%, respectively, while its elastic modulus decreases by 29 and 47%, respectively. Similar to the previous experiment, the decrease in hardness is greater than that in the elastic modulus under different NaCl concentrations.

The analysis above shows that increasing current density and NaCl electrolyte concentration accelerates the degradation of the CF anode, leading to a gradual reduction in fiber hardness. However, the elastic modulus of the CF anode does not decrease at the same rate as the hardness, performing better at lower current densities or electrolyte concentrations. This trend is similar to that observed for hardness. To better understand the varying decline rates of different physical properties during CF anode degradation in electrochemical systems, it is necessary to conduct detailed microscopic analyses and discussion on the impact of functional groups and elemental compositions.

3.2. Influence on Functional Groups and Elemental Compositions. Due to the rapid decrease in hardness and elastic modulus of CF anodes during electrolysis, it is crucial to conduct a thorough investigation of their microscopic chemical composition changes. Therefore, this study explored the differences in functional groups and elemental compositions at various current densities and electrolyte concentrations.

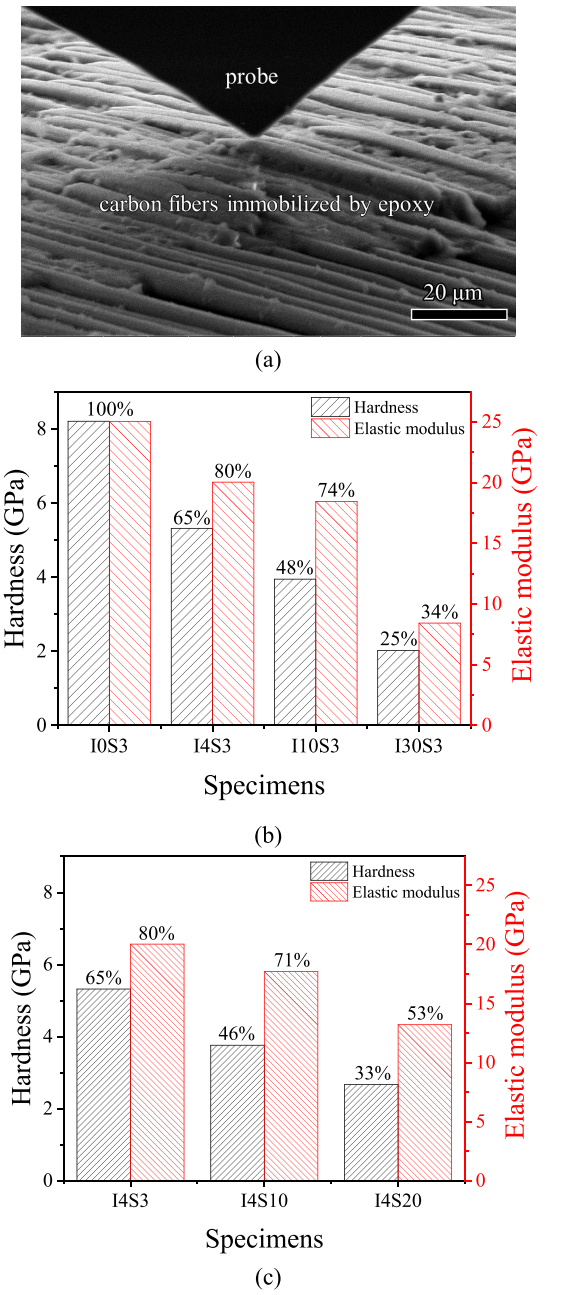

Figure 3. (a) Image of NI probe and CFs immobilized by epoxy during nanoindentation testing, and hardness and elastic modulus of the CF anode energized varying with (b) currents and (c) electrolyte concentrations.

The FTIR method was used to investigate the functional groups present in the CF anode. Figure 4a shows the test results of samples under different current densities when the NaCl electrolyte concentration is kept at 3%. As the current density increases to 7.5 A/m^2, the peaks at 3378, 1728, 1613, 1410, and 550 cm^{-1} in the spectrum of the I30S3 sample become more pronounced. These peaks correspond to the stretching vibration peak of O−H in carboxyl groups (−COOH), the stretching vibration peak of the carbonyl group (−C═O), the stretching vibration peak of C═O in carboxyl groups (−COOH), in-plane bending vibration of

https://doi.org/10.1021/acsomega.3c02900
ACS Omega 2023, 8, 26359−26368

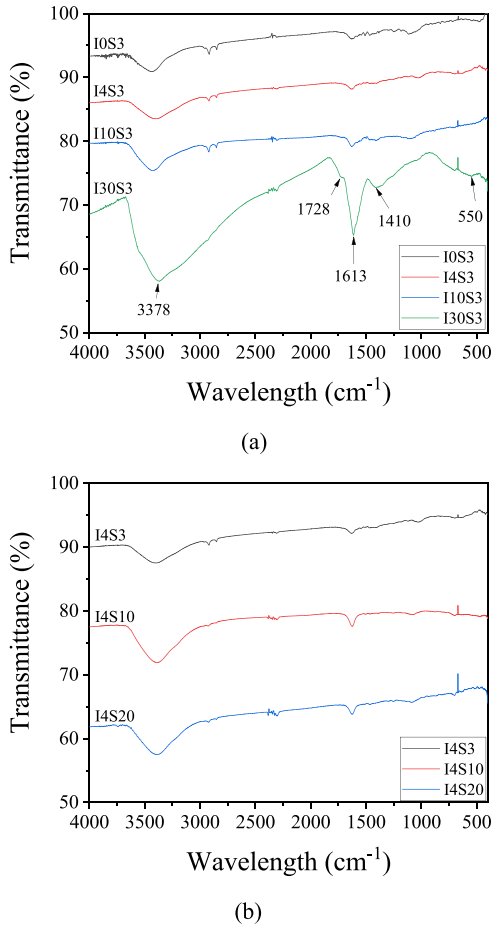

Figure 4. FTIR spectra of CF anodes as a function of current density (a) and electrolyte concentration (b).

hydroxyl groups (−OH), and out-of-plane bending vibration of hydroxyl groups (−OH), respectively.[11] The results suggest that the C−C bond on the surface of the CF anode reacts with water and oxygen ions, leading to continuous oxidation into a large number of carboxyl groups (−COOH), carbonyl groups (−C═O), and hydroxyl groups (−OH).

Figure 4b shows the experimental results of samples under different NaCl electrolyte concentrations when the current density is kept at 1.0 A/m^2. It can be observed that the magnitude of peak intensity variation does not change significantly with increasing NaCl electrolyte concentration (from 3 to 20%). This suggests that the content of the carboxyl group (−COOH), carbonyl group (−C═O), and hydroxyl group (−OH) did not vary significantly with increasing NaCl electrolyte concentration during the electrolysis process. Therefore, the main factor affecting the content of oxygen-containing functional groups in the CF anode is the current density rather than the concentration of NaCl electrolyte.

To verify the inference of functional group changes during the electrolysis process, this study conducted an elemental content analysis of CF anode samples using the EDS analysis method.

Figure 5 illustrates that the oxygen content in CF anode samples increases continuously with increasing current density and NaCl electrolyte concentration. When the current density reaches 7.5 A/m^2, the oxygen content of the CF anode increases by 118.4% compared to the control group. While the oxygen content in the CF anode also increases with increasing NaCl electrolyte concentration, the increase is smaller than that observed with increasing current density. The EDS data are consistent with the abundant presence of oxygen-containing functional groups in the FTIR spectra, which correspond to the continuous decrease in hardness and elastic modulus of individual fibers with increasing current density. These findings suggest a strong correlation between the degradation trend of CF anodes in electrochemical systems and their elemental composition, particularly the oxygen content. Further characterization and analysis of this relationship are necessary.

3.3. Relationship between Mechanical Properties and Elemental Composition. As demonstrated in the previous section, there is a strong correlation between the degradation tendency of CF anodes in electrochemical systems and their oxygen content. Hence, it is imperative to compare and discuss the relationship between them.

Figure 6 illustrates the decrease in various mechanical properties of CF anodes as the oxygen content increases, with NaCl electrolyte concentration kept at 3%. As shown in the figure, when the oxygen content of CF anodes increased from 22.67% (unenergized) to 27.31% (current density 1.0 A/m^2), the reduction degree of their mechanical properties varied significantly. The decreasing order was elongation at break (63%) > hardness (35%) > elastic modulus (20%) > maximum tensile force (12%). These findings suggest that the toughness of the CF anode is greatly reduced and becomes brittle at this stage, but the ultimate tensile strength does not decline

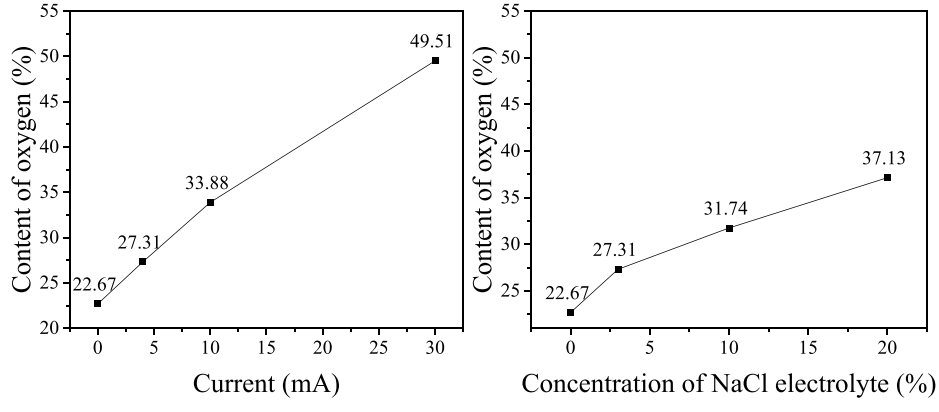

Figure 5. Content of oxygen vs currents and concentration of NaCl electrolyte in CF anodes.

https://doi.org/10.1021/acsomega.3c02900
ACS Omega 2023, 8, 26359−26368

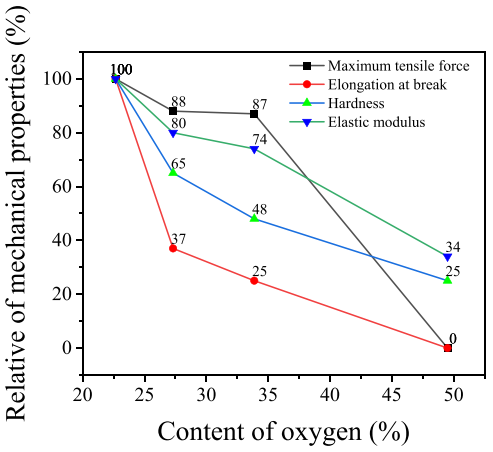

Figure 6. Decline in mechanical properties of CF anodes varying with content of oxygen at constant concentration of NaCl electrolyte (3%).

significantly. Furthermore, the decrease in the hardness of individual fibers is greater than that of the elastic modulus.

As the oxygen content increased to 33.88% (current density 2.5 A/m^2), the elongation at break of CF anodes continued to decrease, while the maximum tensile force remained mostly unchanged. This suggests that the CF anode sample maintained its original tensile strength but became more brittle, with the elastic modulus of individual fibers still decreasing more than the hardness. When the oxygen content further increased to 49.51% (current density 7.5 A/m^2), the elastic modulus and hardness of individual fibers continued to decrease, resulting in the CF anode losing its tensile ability due to longitudinal fiber fracture. Consequently, the elongation at break and maximum tensile force dropped sharply to zero.

Figure 7 illustrates the changes in mechanical properties of CF anodes as the oxygen content increases, with NaCl current

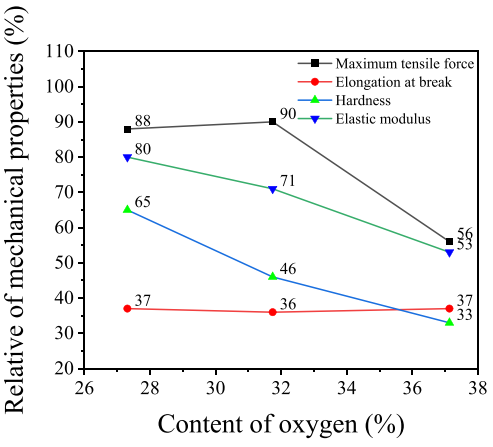

Figure 7. Decline in mechanical properties of CF anodes varying with content of oxygen at constant current density (1.0 A/m^2).

density kept at 1.0 A/m^2. As shown in the figure, when the oxygen content of the CF anode sample increased from 27.31% (NaCl electrolyte concentration 3%) to 31.74% (NaCl electrolyte concentration 10%), its maximum tensile force and elongation at break remained largely unchanged, while the elastic modulus and hardness of individual fibers continued to decrease.

When the oxygen content in the CF anode sample increased from 31.74% (with NaCl electrolyte concentration of 10%) to 37.13% (with NaCl electrolyte concentration of 20%), the elongation at break remained relatively stable, but the maximum tensile force decreased significantly. This suggests that while toughness remains largely unchanged, tensile strength can be greatly reduced, which is the opposite effect of current density increase-induced degradation. Additionally, the elastic modulus and hardness of individual fibers continued to decrease as before.

It is speculated that the degradation of CF anodes in electrochemical systems can be divided into two parts. The first part involves changes to the molecular structure, where an increase in oxygen-containing functional groups breaks the six-membered ring of CF graphite crystallites. Excessive oxidative etching destroys the edges of graphite crystallites, resulting in brittleness of the carbon layer connected to oxygen-containing groups.[12]

The change is noticeable at low current densities (1.0 A/m^2) and increases gradually with current density. Introduction of oxygen-containing groups increases polar adsorption sites and chemical bonding points between molecular interfaces, improving interlaminar shear strength of CFs.[12,13] This improvement is reflected in increased maximum tensile force and individual fiber elastic modulus in this experiment, partially offsetting adverse effects of molecular structure changes on tensile properties. The second part involves erosion of the surface of the CF anode, mainly affecting the surface part of the carbon fiber. Since converted functional groups are hydrophilic, the surface of the CF anode dissolves and falls off with an increasing oxidation degree, generating surface defects and reducing overall mechanical properties.

3.4. Morphological Observation of Single Fibers. To verify the above explanation, SEM images of different CF anodes were taken and are shown in Figure 8. The surface of

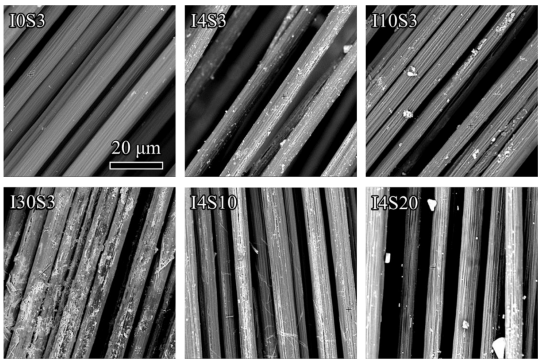

Figure 8. Secondary electron images of CF anodes through EDS.

the unenergized sample (I0S3) is very smooth, reflecting superior mechanical properties of the CF. With increasing current density and NaCl electrolyte concentration in the electrochemical system, cracks and defects on the surface of the CF anode gradually increase, especially evident in the I30S3 sample, consistent with changes in mechanical properties.

The decline in overall mechanical properties of the CF anode is due to both molecular structure changes and surface corrosion. From the aspect of molecular structure change, the C−C bond reacts with water and oxygen ions, leading to the break of the six-membered ring carbon structure and oxidation into carboxyl groups (−COOH), carbonyl groups (−C═O), and hydroxyl groups (−OH). Thus, changes in the molecular

https://doi.org/10.1021/acsomega.3c02900
ACS Omega 2023, 8, 26359−26368

structure lead to a decrease in elongation at break with increasing current density, while the maximum tensile force remains relatively stable due to increased polarity of the molecular structure until longitudinal fibers dissolve and fall off due to excessive surface defects. From the aspect of surface corrosion, cracks and defects on the surface of the CF anode have compromised the integrity of the CF. Increasing NaCl electrolyte concentration has little effect on the molecular structure of the CF anode but increases the area and depth of surface corrosion, resulting in a significant decrease in the maximum tensile force of the CF anode while elongation at break remains basically unchanged for the nonsurface part of individual fibers.

The decline in mechanical properties of individual fibers is a result of simultaneous effects of molecular structure changes and surface corrosion of the CF anode, adversely affected by increasing current density and NaCl electrolyte concentration. Due to increased polarity of the molecular structure, the decrease in the elastic modulus of individual fibers is smaller than that of hardness, with no obvious trend when current density increases from 1.0 to 2.5 A/m^2. At 7.5 A/m^2, the corrosion area and depth of individual fiber surfaces increase significantly, greatly weakening the offset effect caused by polarity of the molecular structure and the negative impact of defects on mechanical properties increases, eventually leading to fracture of the CF anode.

3.5. Investigation on Three-Phase Boundary Regions.

When the CF is utilized as an anode in electrochemical systems, its tendency to fracture frequently can disrupt the electrolysis process and result in avoidable material loss, ultimately reducing the overall recycling efficiency. Thus, it is crucial to identify a viable solution to prevent premature fracture of specific sections of the CF anode.

3.5.1. Region Delineation of the CF Anode. During electrolysis in electrochemical systems, the corrosion of each CF anode is most evident at a specific height above the electrolyte surface, as illustrated in Figure 9. This region, known as the gas/liquid/solid three-phase boundary (TPB) region, exhibits a rough surface and increased brittleness when touched.[14] The TPB region arises due to the higher oxygen concentration in air compared to the electrolyte during electrolysis. This leads to the generation of oxygen ions from the loss of electrons, which dissolve into the interstices between fibers within the TPB region and accelerate the oxidation of the CF anode in this area.[15]

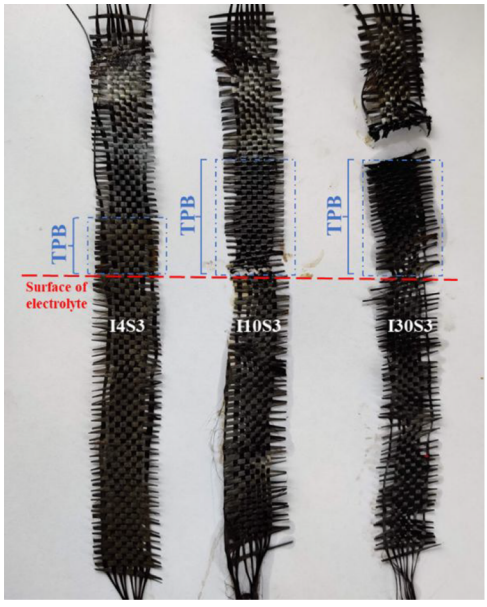

Figure 9. TPB regions in all CF anodes.

Increasing the current density from 1.0 to 2.5 A/m^2 not only doubles the area of the TPB region of the CF anode but also causes fractures at the surface of the electrolyte. The increase in the TPB region's area is due to both capillary action, which causes upward movement of the electrolyte in slender interstices between fibers, and electroosmosis.[16] As the electric field force increases with a higher current density, the electrolyte climbing height also increases. Since the electrochemical reaction takes the longest time at the lower edge, fractures occur first in this area.

At a current density of 7.5 A/m^2, the height of the TPB region of the CF anode remained unchanged but the surface corrosion of the fibers became more severe. The TPB area exhibited disordered fiber surfaces, with indistinguishable contours between transverse and longitudinal fibers, and the position of the first fracture shifted from the lower edge to the upper edge. This illustrates that current density has a direct effect on the degree of CF anode corrosion, with higher current densities resulting in more pronounced corrosion. Capillary action and electroosmosis cause electrolyte climbing until evaporation and replenishment reach a dynamic balance, halting TPB region expansion. However, further testing is required to determine the reason for the change in the CF anode's fracture position.

3.5.2. Difference between the Regions. To gain a better understanding of the differences between the TPB region and non-TPB region on the CF anode and determine why the fracture position changes at varying current densities, this study utilized the most degraded I30S3 sample (current density 7.5 A/m^2) after electrolysis to characterize functional group differences at four locations using the FTIR method.

The FTIR spectrum results, as shown in Figure 10, were obtained from four different locations: 20 mm above the TPB region, the center of the TPB region, 20 mm below the TPB region, and 80 mm below the TPB region. The spectrum measured at the center of the TPB area exhibited five particularly prominent peaks (3378, 1728, 1613, 1410, and 550 cm^{-1}), which correspond to the stretching vibration peak of O−H in carboxyl groups (−COOH), the stretching vibration peak of the carbonyl group (−C═O), the stretching vibration peak of C═O in carboxyl groups (−COOH), in-plane bending vibration of hydroxyl groups (−OH), and out-of-plane bending vibration of hydroxyl groups (−OH), respectively.[11] It can be inferred that on the surface of the TPB region of the CF anode, the C−C bond reacts with water and oxygen ions, leading to continuous oxidation into a large number of carboxyl groups (−COOH), carbonyl groups (−C═O), and hydroxyl groups (−OH). As the number of oxidized C−C bonds increases, defects on the surface of the CF anode become more apparent, ultimately resulting in fracture. A schematic illustration of the oxidative degradation progress of the TPB region in the CF anode is presented in Figure 11.

At a current density of 7.5 A/m^2, the first fracture in the TPB region occurs at the upper edge, indicating that this area experiences the fastest oxidation rate under these electrification conditions. This may be due to capillary action and

https://doi.org/10.1021/acsomega.3c02900
ACS Omega 2023, 8, 26359−26368

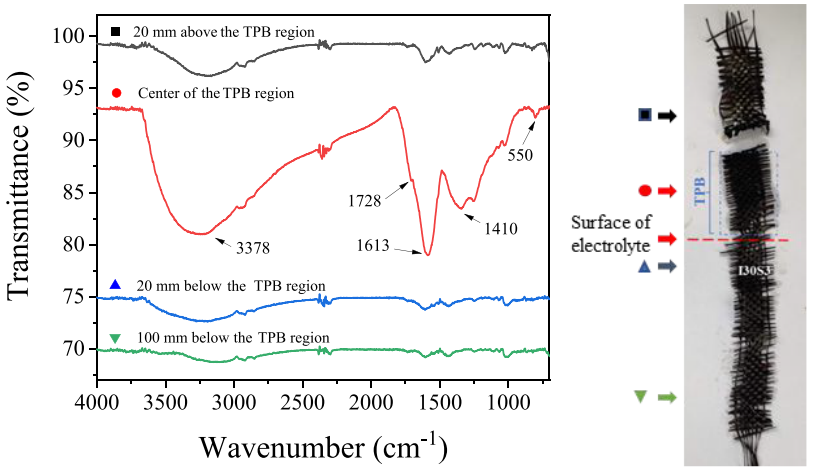

Figure 10. FTIR spectra of the CF anode (I30S3) at different regions.

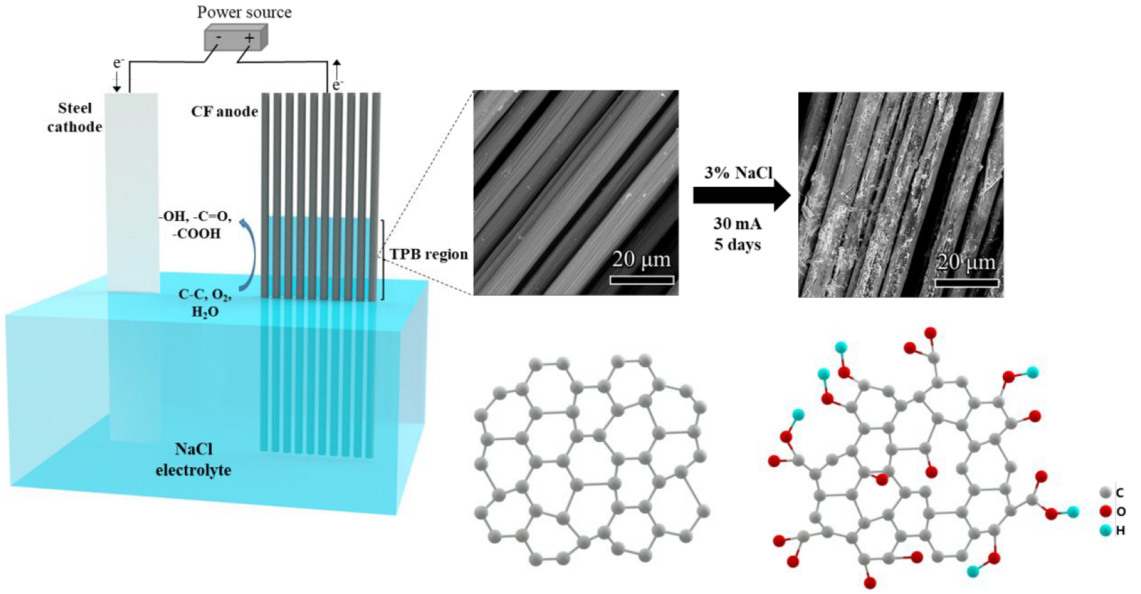

Figure 11. Schematic presentation of the oxidative degradation progress of the TPB region in the CF anode.

electroosmosis, which cause a significant amount of electrolyte absorption in the fiber interstices within the TPB region. During energization, these electrolytes release oxygen through electrolysis, with some escaping directly into air and the rest moving up to the top of the TPB region, resulting in the highest oxygen content in the electrolyte at the upper edge and the most rapid oxidation of the CF anode. When the current density is low, the oxygen content of the electrolyte at the upper edge of the TPB region is not significantly different from other positions due to slower accumulation rates, while the CF at the lower edge undergoes the longest oxidation time and fractures first.

3.5.3. Discussion. To prevent the occurrence of TPB regions in electrochemical systems, the oxygen content of the environment surrounding the CFRP can be reduced by increasing the protective layer thickness or optimizing the epoxy resin proportion to reduce microchannel generation between individual fibers. The functional group changes during degradation are consistent with reactions during electrochemical recycling of waste CFRPs, where the C−C bond reacts with water and oxygen ions, continuously oxidizing into carboxyl groups (−COOH), carbonyl groups (−C═O), and hydroxyl groups (−OH).[6]

The recycling efficiency of the TPB region is higher than other regions during electrochemical progression for recycling waste CFRPs. If fully utilized, this feature can effectively improve the efficiency of electrochemical recycling of waste CFRPs. For instance, gradually moving the CF anode downward during electrification can prevent excessive degradation of the CF anode by avoiding a prolonged stay in the TPB region, which leads to fracture. This implies that if each region of the CF anode can be retained in the TPB region for a sufficient duration and then dissolved into the electrolyte with the aid of oxygen-containing functional groups on its surface, there is a significant potential to enhance the efficiency of electrochemical recycling of waste CFRPs.

4. CONCLUSIONS

The study investigated the degradation mechanism of CF anodes by analyzing changes in their mechanical properties, functional groups, morphological observation, and elemental

https://doi.org/10.1021/acsomega.3c02900
ACS Omega 2023, 8, 26359−26368

composition of individual fibers. The results are summarized below.

- CF anodes underwent significant corrosion during their use in the electrochemical system, as demonstrated by a decrease in tensile strength and ductility, even with a low current density (1.0 A/m^2) and NaCl electrolyte concentration (3%). The TPB region was particularly affected by severe degradation.
- The quantity of oxygen-containing functional groups in the TPB region is the primary factor that influences the degradation performance of CF anodes. This leads to a gradual decrease in the hardness and elastic modulus of individual fibers, ultimately resulting in the fracture of the CF anodes.
- The degradation of the TPB region in CF anodes can be attributed to two primary factors. First, the increase in oxygen-containing functional groups in individual fibers leads to breaks in the six-membered ring of CF graphite crystallites. Second, the surface erosion of CF anodes causes it to gradually dissolve and fall off with stronger oxidation, ultimately resulting in the formation of defects and worsened mechanical properties.
- The degree of degradation in CF anodes is higher with an increase in current density and electrolyte concentration, which can be attributed to the corresponding rise in the oxygen element content.
- If each region of the CF anode can be retained in the TPB region for a sufficient duration and then dissolved into the electrolyte with the aid of oxygen-containing functional groups on its surface, there is a significant potential to enhance the efficiency of electrochemical recycling of waste CFRPs.

AUTHOR INFORMATION

Corresponding Author

Li Ling − *Guangdong Provincial Key Laboratory of Durability for Marine Civil Engineering, College of Civil and Transportation Engineering, Shenzhen University, Shenzhen 518060, China;* orcid.org/0000-0002-1101-6978; Email: popwii90@gmail.com

Authors

Hongfang Sun − *Guangdong Provincial Key Laboratory of Durability for Marine Civil Engineering, College of Civil and Transportation Engineering, Shenzhen University, Shenzhen 518060, China*

Wenpeng Liu − *Guangdong Provincial Key Laboratory of Durability for Marine Civil Engineering, College of Civil and Transportation Engineering, Shenzhen University, Shenzhen 518060, China*

Jie Ren − *Guangdong Provincial Key Laboratory of Durability for Marine Civil Engineering, College of Civil and Transportation Engineering, Shenzhen University, Shenzhen 518060, China*

Chao Wu − *Guangdong Provincial Key Laboratory of Durability for Marine Civil Engineering, College of Civil and Transportation Engineering, Shenzhen University, Shenzhen 518060, China*

Feng Xing − *Guangdong Provincial Key Laboratory of Durability for Marine Civil Engineering, College of Civil and Transportation Engineering, Shenzhen University, Shenzhen 518060, China;* orcid.org/0000-0003-0564-2187

Wei Liu − *Guangdong Provincial Key Laboratory of Durability for Marine Civil Engineering, College of Civil and Transportation Engineering, Shenzhen University, Shenzhen 518060, China*

Complete contact information is available at: https://pubs.acs.org/10.1021/acsomega.3c02900

Notes

The authors declare no competing financial interest.

ACKNOWLEDGMENTS

This research work was financially supported by the National Natural Science Foundation of China (Grant Nos. 52178230, 51878412, 51878413, and 51978408), the Shenzhen R&D Fund (Grant No. JCYJ20190808112019066), and the Guangdong Provincial Key Laboratory of Durability for Marine Civil Engineering (SZU) (Grant No. 2020B1212060074).

REFERENCES

(1) (a) Pham, H. B.; Al-Mahaidi, R.; Saouma, V. Modelling of CFRP−concrete bond using smeared and discrete cracks. *Compos. Struct.* **2006**, *75*, 145−150. (b) Piñero-Hernanz, R.; García-Serna, J.; Dodds, C.; Hyde, J.; Poliakoff, M.; Cocero, M. J.; Kingman, S.; Pickering, S.; Lester, E. Chemical recycling of carbon fibre composites using alcohols under subcritical and supercritical conditions. *J. Supercrit. Fluids* **2008**, *46*, 83−92. (c) Ferrari, A. C.; Basko, D. M. Raman spectroscopy as a versatile tool for studying the properties of graphene. *Nat. Nanotechnol.* **2013**, *8*, 235−246. (d) Yue, L.; Liu, X.; Wu, M. J. C.; Materials, B. Mechanical properties of FRP-strengthened concrete at elevated temperature. *Construct. Build. Mater.* **2017**, *134*, 424−432. (e) Han, P.; Yang, L.; Zhang, S.; Gu, Z. Constructing a Superior Interfacial Microstructure on Carbon Fiber for High Interfacial and Mechanical Properties of Epoxy Composites. *Nanomaterials* **2022**, *12*, 2778. (f) Zhang, Z.; Zhou, J.; Ren, Y.; Li, W.; Li, S.; Chai, N.; Zeng, Z.; Chen, X.; Yue, Y.; Zhou, L.; et al. Passive Deicing CFRP Surfaces Enabled by Super-Hydrophobic Multi-Scale Micro-Nano Structures Fabricated via Femtosecond Laser Direct Writing. *Nanomaterials* **2022**, *12*, 2782. (g) Rehman, S.; Gomez, J.; Villaro, E.; Cossey, D.; Karagiannidis, P. G. Βio-Based Epoxy/Amine Reinforced with Reduced Graphene Oxide (rGO) or GLYMO-rGO: Study of Curing Kinetics, Mechanical Properties, Lamination and Bonding Performance. *Nanomaterials* **2022**, *12*, 222.

(2) Lefeuvre, A.; Garnier, S.; Jacquemin, L.; Pillain, B.; Sonnemann, G. Anticipating in-use stocks of carbon fibre reinforced polymers and related waste generated by the wind power sector until 2050. *Resour. Conserv. Recycl.* **2019**, *141*, 30−39.

(3) (a) Pickering, S. J.; Kelly, R. M.; Kennerley, J. R.; Rudd, C. D.; Fenwick, N. J. A fluidised-bed process for the recovery of glass fibres from scrap thermoset composites. *Compos. Sci. Technol.* **2000**, *60*, 509−523. (b) Ogi, K.; Shinoda, T.; Mizui, M. Strength in concrete reinforced with recycled CFRP pieces. *Compos. A-Appl. Sci. Manuf.* **2005**, *36*, 893−902. (c) Nahil, M. A.; Williams, P. T. Recycling of carbon fibre reinforced polymeric waste for the production of activated carbon fibres. *J. Anal. Appl. Pyrol.* **2011**, *91*, 67−75. (d) Goto, M. Chemical recycling of plastics using sub- and supercritical fluids. *J. Supercrit. Fluids* **2009**, *47*, 500−507. (e) Kim, K. W.; Lee, H. M.; An, J. H.; Chung, D. C.; An, K. H.; Kim, B. J. Recycling and characterization of carbon fibers from carbon fiber reinforced epoxy matrix composites by a novel super-heated-steam method. *J. Environ. Manage.* **2017**, *203*, 872−879. (f) Quach, Q.; Abdel-Fattah, T. M. Silver Nanoparticles Functionalized Nanosilica Grown over Graphene Oxide for Enhancing Antibacterial Effect. *Nanomaterials* **2022**, *12*, 3341. (g) Butenegro, J. A.; Bahrami, M.; Swolfs, Y.; Ivens, J.; Martinez, M. A.; Abenojar, J. Novel Thermoplastic Composites Strengthened with Carbon Fiber-Reinforced

Epoxy Composite Waste Rods: Development and Characterization. *Polymers* **2022**, *14*, 3951. (h) Rabe, D.; Häntzsche, E.; Cherif, C. Recycling of Carbon Fibres and Subsequent Upcycling for the Production of 3D-CFRP Parts. *Materials* **2022**, *15*, 5052. (i) Smoleń, J.; Olesik, P.; Jała, J.; Adamcio, A.; Kurtyka, K.; Godzierz, M.; Kozera, R.; Kozioł, M.; Boczkowska, A. The Use of Carbon Fibers Recovered by Pyrolysis from End-of-Life Wind Turbine Blades in Epoxy-Based Composite Panels. *Polymer* **2022**, *14*, 2925. (j) Stergiou, V.; Konstantopoulos, G.; Charitidis, C. A. Carbon Fiber Reinforced Plastics in Space: Life Cycle Assessment towards Improved Sustainability of Space Vehicles. *J. Compos. Sci.* **2022**, *6*, 144.

(4) (a) Kumar, S.; Krishnan, S. Recycling of carbon fiber with epoxy composites by chemical recycling for future perspective: a review. *Chem. Pap.* **2020**, *74*, 3785−3807. (b) Amamoto, Y.; Kamada, J.; Otsuka, H.; Takahara, A.; Matyjaszewski, K. Repeatable photoinduced self-healing of covalently cross-linked polymers through reshuffling of trithiocarbonate units. *Angew. Chem. Int. Ed.* **2011**, *123*, 1698−1701. (c) Yu, K.; Shi, Q.; Dunn, M. L.; Wang, T.; Qi, H. J. Carbon fiber reinforced thermoset composite with near 100% recyclability. *Adv. Funct. Mater.* **2016**, *26*, 6098−6106.

(5) (a) Ogi, K.; Nishikawa, T.; Okano, Y.; Taketa, I. Mechanical properties of ABS resin reinforced with recycled CFRP. *Adv. Compos. Mater.* **2007**, *16*, 181−194. (b) Liu, Y.; Liu, J.; Jiang, Z.; Tang, T. Chemical recycling of carbon fibre reinforced epoxy resin composites in subcritical water: Synergistic effect of phenol and KOH on the decomposition efficiency. *Polym. Degrad. Stabil.* **2012**, *97*, 214−220. (c) Yang, Y.; Boom, R.; Irion, B.; van Heerden, D.-J.; Kuiper, P.; de Wit, H. Recycling of composite materials. *Chem. Eng. Process.: Process Intesif.* **2012**, *51*, 53−68. (d) Pimenta, S.; Pinho, S. T. Recycling carbon fibre reinforced polymers for structural applications: technology review and market outlook. *Waste Manage.* **2011**, *31*, 378−392. (e) Liu, W.; Huang, H.; Zhu, L.; Liu, Z. Integrating carbon fiber reclamation and additive manufacturing for recycling CFRP waste. *Composites, Part B* **2021**, *215*, No. 108808. (f) Ling, L.; Wu, C.; Xing, F.; Memon, S. A.; Sun, H. Recycling Nanoarchitectonics of Graphene Oxide from Carbon Fiber Reinforced Polymer by the Electrochemical Method. *Nanomaterials* **2022**, *12*, 3657. (g) Centi, G.; Perathoner, S. Opportunities and prospects in the chemical recycling of carbon dioxide to fuels. *Catal. Today* **2009**, *148*, 191−205. (h) Olah, G. A. Efficient and selective chemical recycling of carbon dioxide to methanol, dimethyl ether and derived products. US12/537,647, 2009. (i) Yan, C.; Lin, D.; Meng, X.; Wen, Z.; Wang, C.; Wang, Y.; Song, Z.; Li, L.; Crittenden, J. C. Closed-Loop Electrochemical Recycling of Spent Copper(II) from Etchant Wastewater Using a Carbon Nanotube Modified Graphite Felt Anode. *Environ. Sci. Technol.* **2018**, *52*, 5940. (j) Zeng, F.; Sun, Z.; Sang, X.; Diamond, D.; Lau, K. T.; Liu, X.; Su, D. S. In Situ one-step electrochemical preparation of graphene oxide nanosheet-modified electrodes for biosensors. *ChemSusChem* **2011**, *4*, 1587−1591. (k) Sukanto, H.; Raharjo, W. W.; Ariawan, D.; Triyono, J. Carbon fibers recovery from CFRP recycling process and their usage: A review. In *IOP Conference Series: Materials Science and Engineering*; IOP Publishing: 2021; Vol. *1034*, p. 012087.

(6) Sun, H.; Guo, G.; Memon, S. A.; Xu, W.; Zhang, Q.; Zhu, J.-H.; Xing, F. Recycling of carbon fibers from carbon fiber reinforced polymer using electrochemical method. *Compos. A-Appl. Sci. Manuf.* **2015**, *78*, 10−17.

(7) (a) Zhang, Y.; Zhang, Y.; Liu, Y.; Wang, X.; Yang, B. A novel surface modification of carbon fiber for high-performance thermoplastic polyurethane composites. *Appl. Surf. Sci.* **2016**, *382*, 144−154. (b) Andideh, M.; Esfandeh, M. Statistical optimization of treatment conditions for the electrochemical oxidation of PAN-based carbon fiber by response surface methodology: Application to carbon fiber/epoxy composite. *Compos. Sci. Technol.* **2016**, *134*, 132−143.

(8) Zhou, Y.; Zheng, X.; Xing, F.; Sui, L.; Zheng, Y.; Huang, X. Investigation on the electrochemical and mechanical performance of CFRP and steel-fiber composite bar used for impressed current cathodic protection anode. *Constr. Build. Mater.* **2020**, *255*, No. 119377.

(9) (a) Sun, H.; Wei, L.; Zhu, M.; Han, N.; Zhu, J.-H.; Xing, F. Corrosion behavior of carbon fiber reinforced polymer anode in simulated impressed current cathodic protection system with 3% NaCl solution. *Constr. Build. Mater.* **2016**, *112*, 538−546. (b) Cheng, H.; Huang, H.; Zhang, J.; Jing, D. Degradation of carbon fiber-reinforced polymer using supercritical fluids. *Fiber Polym.* **2017**, *18*, 795−805.

(10) Kaynak, A.; Polat, A.; Yilmazer, U. Some microwave and mechanical properties of carbon fiber-polypropylene and carbon black-polypropylene composites. *Mater. Res. Bull.* **1996**, *31*, 1195−1206.

(11) (a) Colthup, N. B. D.; Daly, L. H.; Wiberley, S. E. *Introduction to Infrared and RAMAN Spectroscopy*; Elsevier, 1964. (b) Pretsch, P. D. D. E.; Clerc, P. D. T.; Seibl, P. D. J.; Simon, P. D. W. *Tables of Spectral Data for Structure Determination of Organic Compounds*; Springer Science & Business Media, 1983. (c) Shin, S.; Jang, J.; Yoon, S. H.; Mochida, I. A study on the effect of heat treatment on functional groups of pitch based activated carbon fiber using FTIR. *Carbon* **1997**, *35*, 1739−1743.

(12) Bogoeva-Gaceva, G.; Burevski, D.; Dekanski, A.; Janevski, A. The effect of surface treatment on the interfacial properties in carbon fibre/epoxy matrix composites. *J. Mater. Sci.* **1995**, *30*, 3543−3546.

(13) Yuan, H.; Wang, C.; Zhang, S.; Lin, X. Effect of surface modification on carbon fiber and its reinforced phenolic matrix composite. *Appl. Surf. Sci.* **2012**, *259*, 288−293.

(14) (a) Deng, H.; Zhou, M.; Abeles, B. Diffusion-reaction in mixed ionic-electronic solid oxide membranes with porous electrodes. *Solid State Ionics* **1994**, *74*, 75−84. (b) Jiang, J.; Wang, J.; Wang, W.; Zhang, W. Modeling influence of gas/liquid/solid three-phase boundary zone on cathodic process of soil corrosion. *Electrochim. Acta* **2009**, *54*, 3623−3629. (c) Jiang, J.; Wang, J.; Lu, Y.-H.; Hu, J.-Z. Effect of length of gas/liquid/solid three-phase boundary zone on cathodic and corrosion behavior of metals. *Electrochim. Acta* **2009**, *54*, 1426−1435.

(15) Adler, S. B.; Lane, J. A.; Steele, B. C. H. Electrode Kinetics of Porous Mixed-Conducting Oxygen Electrodes. *J. Electrochem. Soc.* **1996**, *143*, 3554−3564.

(16) Acar, Y. B.; Alshawabkeh, A. N. Principles of electrokinetic remediation. *Environ. Sci. Technol.* **1993**, *27*, 2638−2647.

https://doi.org/10.1021/acsomega.3c02900
ACS Omega 2023, 8, 26359−26368